Age-related Changes of the Traction-separation Law Parameters for the Description of the Delamination of the Human Aorta

Lukáš Horný[1, a)], Zdeněk Petřivý[1, b)], Petr Tichý[1, c)], Hynek Chlup[1, d)], Jakub Kronek[1, e)], Tomáš Adámek[2, f)] and Alžběta Blanková[2, g)]

[1]*Czech Technical University in Prague, Faculty of Mechanical Engineering, Technická 4, 160 00 Prague, Czech Republic.*
[2]*Regional Hospital Liberec, Department of Forensic Medicine and Toxicology, Husova 357/10, 460 63 Liberec, Czech Republic.*

[a)] *Corresponding author: lukas.horny@fs.cvut.cz*
[b)]*zdenek.petrivy@cvut.cz*
[c)]*petr.tichy@fs.cvut.cz*
[d)]*hynek.chlup@fs.cvut.cz*
[e)]*jakub.kronek@fs.cvut.cz*
[f)]*tomas.adamek@nemlib.cz*
[g)]*alzbeta.blankova@nemlib.cz*

Abstract. Aortic dissection is a life-threatening disease manifested by a tear that separates the aortic wall into two layers. The mechanical conditions under which delamination of the human aorta occurs are the subject of our study. Our study combines experimental and computational approaches. Delamination strength is investigated in the peeling experiments, which resemble the mode I crack opening well-known from fracture mechanics. Peeling experiments were designed to take into account the possible effects of the material anisotropy and site-specific differences in the mechanical properties that occur along the aortic length. The computational branch of our study is based on the FEM model of the peeling experiment built in Abaqus and attempts to find the location-dependent parameters of the traction-separation law that would reflect age-related changes in delamination resistance. Our results suggest that there is a strong correlation between age and delamination strength which is expressed by the age-specific values of the material parameters that characterize the delamination interface.

INTRODUCTION

Arterial dissection is a life-threatening disease manifested by a separation of the layers of an artery wall [1–3]. It occurs most frequently in the thoracic part of the aorta, but it can spread along its entire length. The dissections of other arteries, like the carotid artery or vertebral artery, are also described in the literature. Although one could consider aortic dissection to be a relatively rare disease, the rate of incidence is typically reported as ranging from 3 to 6 cases per 100 000 per year, nevertheless the lethality of acute dissection is rather high. According to [4], 37% of patients who reach the hospital alive die within the next 30 days, and approximately 20% of patients die before they receive medical intervention [5].

During dissection, blood enters the wall and causes the delamination of its layers. Further separation often leads to the creation of a new false lumen which can extend longitudinally. The dissection tear may run along an artery, along with some radial inclination, and reach the external surface of the artery. In such a case, internal hemorrhage

follows. Another kind of failure induced by the dissection is a rupture of the weakened cross-section of the dissected artery wall.

Thus far, the exact dissection-initiation mechanism has not been definitively established and a detailed description of dissection propagation is the subject of current research. Our study tries to extend the knowledge of the biomechanics of aortic delamination by means of both experimental and computational approaches. The peeling experiment is the basic instrument utilized to show how the delamination strength depends on the anatomical site, loading speed and crack tip orientation, and how the delamination resistance depend on age. The computational branch of our study is based on the FEM model of the delamination test built in Abaqus. It attempts to find the age and location-dependent parameters of the traction-separation law of a cohesive interface. In this paper, we show what parameters a linear model of the traction-separation could have in the case of the human thoracic ascending aorta.

METHODS

Samples

Segments of human aortas were obtained during regular autopsies conducted in the Department of Forensic Medicine and Toxicology at the Regional Hospital Liberec. The post-mortem use of human tissue was approved by the Ethics Committee of the Regional Hospital Liberec. Highly calcified segments and tissues from cadavers exhibiting putrefaction changes were not included in the study. Any possible bias in the results due to post-mortem changes was ruled out by post-hoc statistical analysis.

Rectangular samples, approx. 8 x 40 mm, were cut from the aortic segments. These segments were excised from the ascending part of the thoracic aorta. In the present paper, we will restrict our attention to samples aligned with the circumferential axis of the aorta.

Delamination experiment

The method adopted to characterize the delamination properties of the aorta was the so-called peeling test. This experimental protocol was, in the context of the biomechanics of aortic dissection, introduced by Sommer et al. in 2008 [1] and has been used in further studies focused on the delamination properties of arteries [6–12]. It resembles the mode I crack opening that is widely used in fracture mechanics, see Fig. 1. The main advantage of this experimental technique lies in the controllable crack propagation, which allows for the quantification of the delamination strength, S_d, defined as the delamination force per the reference width.

As indicated in Fig. 1, when the clamps move apart, the forces induced by them open the crack front and delamination takes place. The intact portion of the sample shortens as the clamps continue in their movement. In the final stage of the experiment, the tested sample falls apart into two separate sections.

The experiments were carried out with the help of the multipurpose tensile testing machine, Zwick/Roell (Messphysik). Both the delamination force F (the force that is necessary to increase a tear length) and the tear length were recorded on a PC. The delamination force was measured by HBM U9C +/- 25N force transducers. The tear length was determined from the movement of the clamps, which was recorded at 1 μm resolution. This data was complemented with the recordings carried out by a built-in video-extensometer, which measured the distance between the marks made on the surface of the samples. In order to determine whether delamination strength depends on loading rate, the experiments were carried out with the clamps' velocity set to 0.1, 1, 10, 50 mms^{-1}.
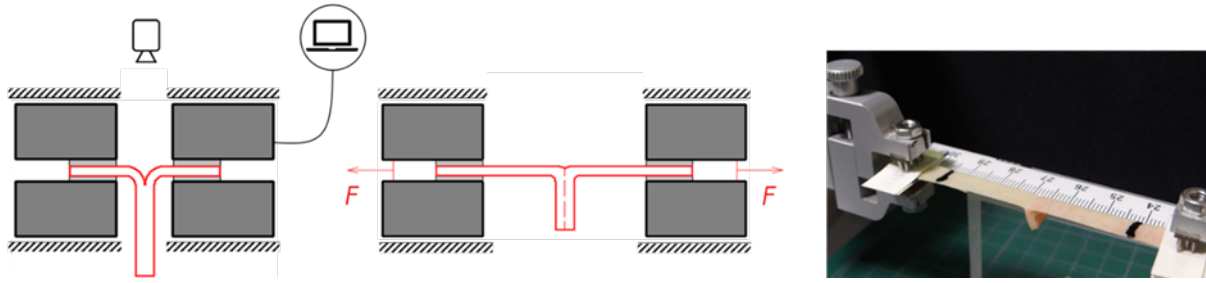
FIGURE 1. Peeling experiment. The left sketch depicts the arrangement of the peeling experiment in our experimental setup where the extension of the sample is recorded by videoextensometer, and loading force, F, is recorded into a PC. The middle sketch illustrates the loaded sample. The photograph on the right shows the real sample within the experiment.

Statistical analysis

The dependence on loading rate was investigated. The Kruskal-Wallis test was employed to test the hypothesis that the collected data does not have different medians when arranged in groups according to the applied loading speed. Non-parametric ANOVA was complemented with the Dunn test to determine which particular groups significantly differ from each other. The hypothesis that the delamination properties depend on age was evaluated in the post-hoc correlation analysis. A classical linear regression model was used to express the regression equation. The Pearson correlation coefficient R was computed and the hypothesis $R = 0$ tested, based on the classical *T-test*. In all statistical evaluations, the results were considered significant at the level $\alpha = 0.05$.

Outline of the regression analysis of the traction-separation law

The principle idea is to simulate the peeling experiments by means of the FEM (or XFEM) used to capture discontinuity propagation. When the geometrical and bulk properties of arterial strips are known, the only unknowns that remain to be determined are the parameters of the traction-separation law. Our FEM model was built in Abaqus (v. 2019, [13]). The delamination interface was modeled via surface-based cohesive behavior. The linear traction-separation law was adopted from [13, 14] and used to describe the properties of the cohesive interface, eq. (1). Here $t = (t_n, t_s, t_t)^T$ is the nominal traction stress vector, $\delta = (\delta_n, \delta_s, \delta_t)^T$ is the separation vector, and K_{ij} ($i,j = n, s, t$) are parameters describing traction-separation stiffness. The default K_{ii} values offered by Abaqus were used (K_{ij} for $i \neq j$ were considered zero).

$$\begin{pmatrix} t_n \\ t_s \\ t_t \end{pmatrix} = \begin{pmatrix} K_{nn} & K_{ns} & K_{nt} \\ K_{ns} & K_{ss} & K_{st} \\ K_{nt} & K_{st} & K_{tt} \end{pmatrix} \begin{pmatrix} \delta_n \\ \delta_s \\ \delta_t \end{pmatrix}$$

(1)

The damage initiation criterion of the maximum separation was used to express the conditions of local failure initiation caused by the delamination process. The criterion is expressed in (2). δ_i^0 ($i = n, s, t$) are separations at which initiation of the damage occurs and were the subjects of our regression analysis of the experimental data. This was based on a comparison of the experimentally measured force required for the delamination process to occur and the reaction force calculated by the FEM model at the reference points (points where the kinematic boundary condition was applied). For the sake of simplicity, $\delta_n^0 = \delta_s^0 = \delta_t^0$ assumption was considered. [] denotes the Macaulay bracket. The evolution of the damage was considered linear, with the maximum plastic displacement assigned to be 0.0002 mm.

$$max \left\{ \frac{[\delta_n]}{\delta_n^0}, \frac{\delta_s}{\delta_s^0}, \frac{\delta_t}{\delta_t^0} \right\} = 1$$

(2)

The entire FEM model consisted of 1000 C3D8IH (3D solid, hybrid formulation, incompatible modes) elements that covered the model of the experimental sample of the following dimensions: 10 mm x 0.1 mm x 1 mm (length x width x height). There was an initial tear created at the mid-height of the specimen model, which was 7 mm long. Figure 2 shows the FEM model.

Bulk material model

Data for the bulk material of the human thoracic ascending aorta were adopted from our previous study. They were based on uniaxial tensile tests conducted with strips obtained from a 76-year-old male donor. The strips were aligned with the circumferential and longitudinal directions of the aorta and underwent coupled regression analysis to take into account material anisotropy. The mechanical response of the aorta was considered to be hyperelastic. The strain energy density model W proposed by Gasser et al. [15] was used. Its specific form is in (3).

$$W = \tfrac{1}{2}\mu\left(\lambda_R^2 + \lambda_\Theta^2 + \lambda_Z^2 - 3\right) + \frac{k_1}{k_2}\left(e^{k_2\left(\kappa\left(\lambda_R^2+\lambda_\Theta^2+\lambda_Z^2\right)+(1-3\kappa)\left(\lambda_\Theta^2\cos^2\beta+\lambda_Z^2\sin^2\beta\right)-1\right)^2} - 1\right)$$

(3)
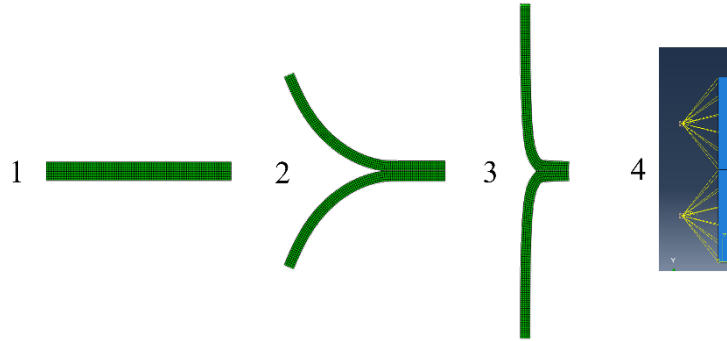
FIGURE 2. FEM model of the peeling experiment. Panel 1 depicts mesh of the model in the reference configuration. Panel 2 depicts mesh in the elastic phase of the loading. Panel 3 depicts the model when the separation takes place. Panel 4 shows tie bonds of the reference points to apply kinematic boundary conditions (displacement in the vertical direction).

In (3), μ, k_1, k_2, β, and κ denote material parameters that, according to the previous experiments, were found to be $\mu = 0.042$ MPa, $k_1 = 4.61$ MPa, $k_2 = 76.9$, $\beta = 0.841$, and $\kappa = 0.191$. λ_R, λ_Θ, and λ_Z are principal stretches in the direction of the radial, circumferential and axial axis of the aorta in its cylindrical configuration. The bulk material was considered to be incompressible. The parameters of W correspond to a 76-year-old individual. In order to estimate the traction separation law parameters for a young individual, parameter k_1 was reduced tenfold and the resulting response was considered to correspond to a 30-year-old individual. At this point, we would like to emphasize that we proceeded in this way only for the purpose of our simulation, designed to verify that traction-separation parameters can reflect changes due to aging. In order to determine the actual parameters, an experiment would need to be performed with tissue from a 30-year-old donor. The uniaxial stress-strain relationships corresponding to the bulk material models used in our study are depicted in Fig. 3.
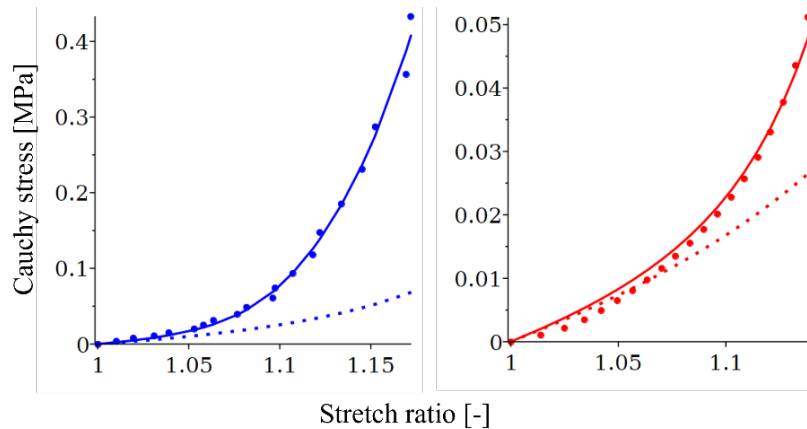
FIGURE 3. Uniaxial stress responses of the aortic strips. The sample aligned with the longitudinal direction is in the left panel, while the right panel shows a circumferentially oriented strip. Experimental data obtained with samples from a 76-year-old donor are depicted by solid circles, and corresponding model responses are depicted with solid curves. The dotted curves correspond to the young individual. This was obtained by reducing the k_1 parameter tenfold.

RESULTS AND DISCUSSION

Delamination experiments

A total number of 107 peeling experiments were carried out. 33 samples were tested at a speed of 0.1 mms^{-1}, 36 at 1 mms^{-1}, 20 at 10 mms^{-1}, and 18 at 50 mms^{-1}. Figure 4 shows box-plots of the resulting delamination forces S_d (per reference width, Nmm^{-1}). The Kruskal-Wallis test did not reveal significant differences in the medians within the investigated groups (*p-value* = 0.32). Hence it was concluded that delamination strength does not depend on the loading rate. This conclusion should be understood as valid within the extent of our observation given by the crack propagation speed from 0.1 mms^{-1} to 50 mms^{-1}.
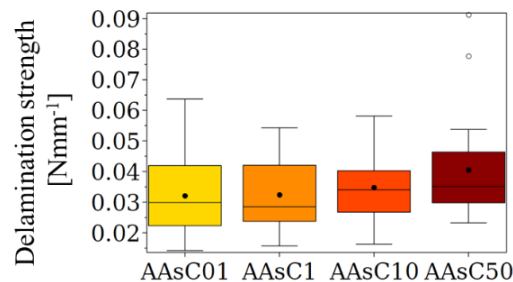
FIGURE 4. Box-plot comparing delamination strengths obtained at different loading rates. The differences were not found to be significant.

Since the hypothesis of the insensitivity of S_d to the extension rate has been accepted, data gained at different speeds were pooled. Therefore, the regression analysis of the dependence of S_d on age, expressed by the linear equation $S_d = a \cdot \text{Age} + b$, was based on all 107 observations. The regression equation parameters were identified in the least squares minimization as a = -0.00033 Nmm^{-1}year^{-1}, and b = 0.054 Nmm^{-1}. The regression line and the collected data points are depicted in Fig. 5. The correlation coefficient between age and delamination strength attained R = -0.35 and was found to be statistically significant (*p-value* < 0.01). It was concluded that delamination resistance is age-dependent and that it significantly decreases with age, which suggests that age is an important risk factor in aortic dissection.
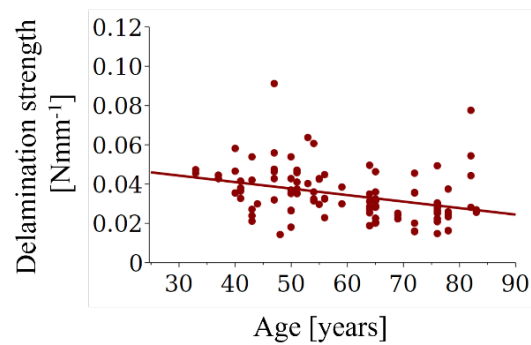
FIGURE 5. Age-related changes of delamination strength. The regression equation predicts $Sd = 0.0441$ Nmm^{-1} at 30 years of age and 0.0289 Nmm^{-1} at 76 years.

Traction-separation law parameters

Another goal of our study was to verify whether the traction-separation law parameters can reflect aging-induced changes in the delamination properties of the aorta. With the help of the heuristic iteration process, the maximum normal separation parameter δ_n^0 was found for the thoracic ascending aorta of 30-year-old (bulk material simulated) and 76-year-old (bulk material based on experiment) men. These parameters were found by means of the FEM model based on the surface-based contact approach. $\delta_n^0 = 5.52\text{E-}5$ mm for a 30-year-old, and $\delta_n^0 = 5.26\text{E-}5$ mm for a 76-year-old individual. Both cases resulted in less than a 1% relative error between the delamination force predicted by the FEM model and S_d predicted by the regression equation described above. The calculated reaction force (per reference width) predicted by FEM is depicted in Fig. 6 where it is plotted as the function of the displacement applied as the boundary condition.
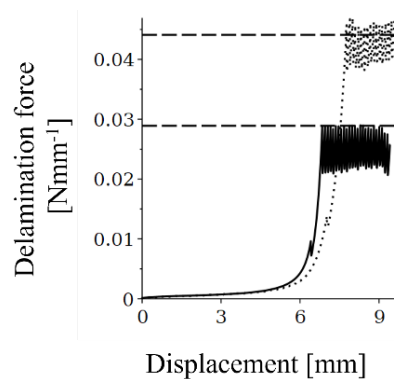
FIGURE 6. The FEM model calculated reaction force required to delaminate arterial strips. The solid curve corresponds to a 76-year-old individual, and the dotted curve corresponds to a 30-year-old. Delamination strengths predicted by the regression equation are depicted by dashed lines.

Limitations of our study

The results shown in the present article represent a pilot study of the procedure to identify the parameters of the traction-separation law. It shows results that should be considered provisional and do not have the ambition to capture aging-induced changes in the delamination mechanics of the human aorta in their full complexity. Several simplifications were adopted in our study and therefore the resulting parameters of the maximum separation criterion

should be treated with caution. In particular, the constitutive description for the bulk material at various stages of aging has to be based on real experiments in the future. In the future, it will also be necessary to complement our study with an anisotropic traction-separation model, as experiments show that delamination strength depends on the orientation of the sample with respect to the blood vessel axes.

CONCLUSIONS

Our experiments did not suggest that the delamination strength of the human aorta would depend on the loading rate. On the other hand, it was concluded that the delamination strength depends on age. For the human thoracic ascending aorta, this dependence was well described by a linear regression equation. The results of the FEM simulation show that the parameters of the maximum separation criterion can reflect age-related changes in delamination strength.

ACKNOWLEDGMENTS

REFERENCES

1. G. Sommer, T.C. Gasser, P. Regitnig, M. Auer and G.A. Holzapfel, J. Biomech. Eng. **130**, art. no. 021007 (2008).
2. C.A. Nienaber and R.E. Clough, The Lancet **385**, 800–811 (2015).
3. T.-Y. Yeh, C.-Y. Chen, J.-W. Huang, C.-C. Chiu, W.-T. Lai and Y.-B. Huang, Medicine **94**, art. no. e1522 (2015).
4. C. Olsson, S. Thelin, E. Ståhle, A. Ekbom and F. Granath, Circulation **114**, 2611–2618 (2006).
5. I. Mészáros, J. Mórocz, J. Szlávi, J. Schmidt, L. Tornóci, L. Nagy, L. Szép, Chest **117**, 1271–1278 (2000).
6. J. Tong, T. Cohnert, P. Regitnig, J. Kohlbacher, R. Birner-Gruenberger, A.J. Schriefl, G. Sommer and G.A. Holzapfel, J. Biomech. **47**, 14–23 (2014).
7. Y. Wang, J.A. Johnson, F.G. Spinale, M.A. Sutton and S.M. Lessner, Exp. Mech. **54**, 677–683 (2014).
8. M. Kozuń, M. Kobielarz, A. Chwiłkowska and C. Pezowicz, J. Mechan. Behav. Biomed. Mater. **79**, 292–300 (2018).
9. M. Kozuń, J. Theor. App. Mech. **54**, 229–238 (2016).
10. M. Kozuń, T. Płonek, M. Jasiński and J. Filipiak, Acta Bioeng. Biomech. **21**, 127-134 (2019).
11. J.C. Chung, E. Wong, M. Tang, D. Eliathamby, T.L. Forbes, J. Butany, C.A. Simmons and M. Ouzounian, J. Am. Heart Assoc. **9**, art. no. e016715 (2020).
12. D.C. Angouras, E.P. Kritharis and D.P. Sokolis, J. Mechan. Behav. Biomed. Mater. **98**, 58-70 (2019).
13. Dassault Systemes. *Documentation to Abaqus 2019 version*. (2019), Available online from https://help.3ds.com
14. A. Ferrara and A. Pandolfi, Int. J. Frac. **166**, 21-33 (2010).
15. T.C. Gasser, R.W. Ogden and G.A. Holzapfel, J. Royal Soc. Interface **3**, 15-35 (2006).